A Novel Axial Flux Stator and Rotor Dual Permanent Magnet Machine

Y. C. Wang, W. N. Fu, and X. J. Li

Abstract—A novel structure of axial flux stator and rotor dual PMs Vernier machine is presented as an effective option for high torque-density direct-driven applications. The key is to locate PMs on both sides of rotor and stator. With dual PMs, this proposed machine with a novel structure generates an improved torque per armature current at low speed. It is very suitable for direct drive applications with limited space such as the in-wheel electric vehicle (EV) motors. The theory of the structure with PMs on both sides is analyzed theoretically. The structure and operation principle of machine are introduced and the steady and steady performance of machine is analyzed and verified with time-stepping finite element method (TS-FEM).

Index Terms—Direct-drive, finite element method, flux modulation, high torque density, permanent magnets

I. INTRODUCTION

D UE to the dramatical improvement of the performance of permanent magnet (PM) materials, PM machines have been applied in more and more application fields, ranging from industrial field such as wind power generator, electrical vehicles to domestic appliances [1-3]. PM machines owns many obvious merits including high efficiency and high power density, over many other electric-excited machines. PM machines can be classified as gear box based type and direct-drive type. For the former one, a reduction gear is always essential for traditional drive systems because of the mismatching between the drive system and the load. However, the mechanical reduction gears bring some additional problems such as mechanical vibration, noise and maintenance cost. To get rid of the reduction gears, direct-drive PM machine is one of the research directions for morden drive systems. Various topologies of the PM machines have been proposed in the past decades years to be desgined as direct-drive machines [4-7]. PM vernier machines as one special case of flux modulation machines are extremely suitable for the low-speed high-torque-density direct-drive system.

Vernier motor structure was proposed firstly by Lee [8] in 1963. Since the PM machine was not popular, the first Vernier motor is a reluctance-type inductor synchronous motor. The PM Vernier machine (PMVM) with high performance PM materials has the feature of high torque at low speed [9-12].

PMVM is also one type of magnetic geared machine machines or flux modulating machines due to the inherent magnetic gear effect. The Vernier structure of PMVM amplifies several specific space harmonics of magnetic field with modulation of uneven air-gap permeance in the air-gap. With the interaction between these specific harmonics and magnetic field excited with rotor PMs, the PMVM produces large torque at low speed. For the conventional PM synchronous machines (PMSM), the stator windings and rotor PM have same poles number. However, in the PMVM, the pole number of stator windings and the rotor PMs are different. The gear ratio of the PMVM is dependent on the selection of the poles number of the rotor PMs (Z_r) and poles number of the stator windings (p). The gear radio is always much greater than one which means p is always designed much smaller than Z_r.

Axial-flux permanent-magnet machines (AFPMM) have been studied for several decades [13-15]. The extreme axial compactness of the AFPMM is its major advantage, which make it very suitable for the space limited applications, such as used as in-wheel motors for the electrical vehicles (EV) and wind power generators. Based on the structure, AFPMMs can be divided into single-stator, single-rotor, double-stator, single-rotor, single-stator, double-rotor and multi-stack structures. For the single-stator, double-rotor machines, the windings can be wounded as ring windings which are also known as back to back or core-wound windings. Compared with traditional tooth-wound windings, the ring windings have excellent performance since the end connection is shorter and the winding utilization is higher. Fig. 1(a) shows the single-stator, double-rotor topology with core-wound windings and NN PMs. The NN indicates that opposing magnets are of same polarity. Fig. 1(b) shows the single-stator, double-rotor topology with core-wound windings and NS PMs. The NS indicates that opposing magnets are of opposite polarity.

In this paper, a novel axial flux dual permanent magnets (AFDPM) machine is proposed. The AFDPM machine adapts single-stator, double-rotor NN structure and core-wound windings as shown in Fig. 2. The basic operating theory of the AFMPMM is that it employs flux modulating effect to integrate the magnetic gear and permanent magnet synchronous machine (PMSM) compactly. With 3d finite

element method (FEM), the theory is verified and the performance of the novel structure is analyzed. A conventional axial flux vernier PM machine (AFVPM) with similar rated speed and volume is studied to compare with the AFDPM machine in term of the torque density. With PMs on both sides of the air-gap, the torque density of the AFDPM machine is improved dramatically when compared with conventional direct-drive machines.
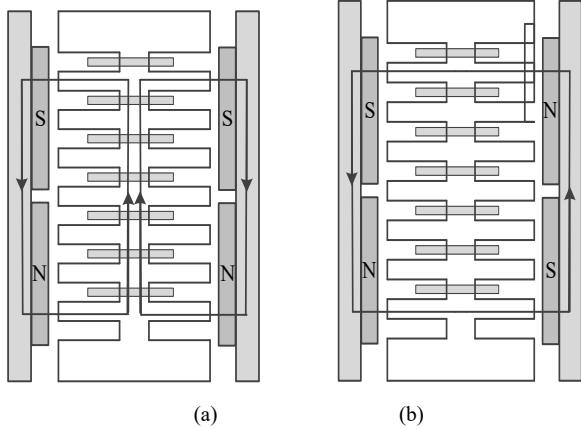

(a)   (b)

Fig. 1. The structure of single stator-double rotor. (a) core-wounding with NN PMs. (b) core-wounding with NS PMs.
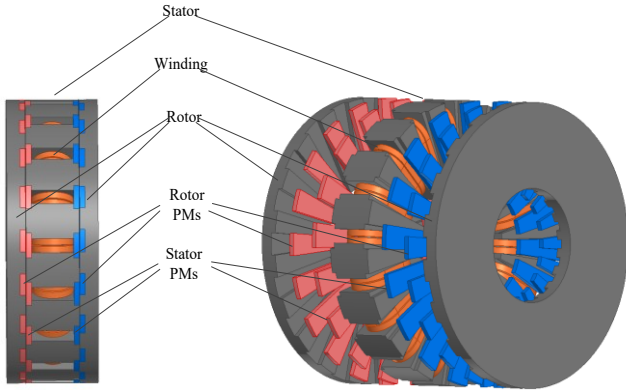

Fig. 2. The structure of the AFMPMM.

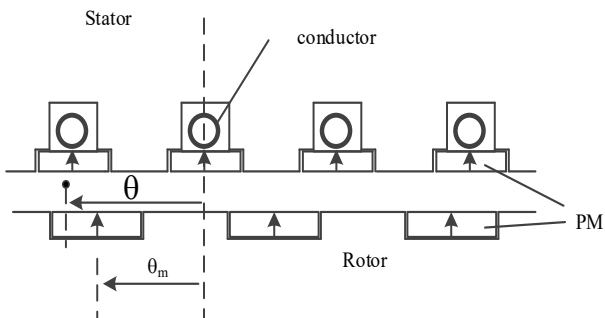## II. OPERATING PRINCIPLE OF DUAL PM FLUX MODULATION MACHINE

Fig. 3. Portion of axial flux stator and rotor dual PM machine.

To illuminate the theory of the AFDPM machine, a portion of the cross section of the axial flux stator and rotor dual PM machine is shown in Fig. 3. To simplify the 3d model to a 2d diagram, the arc is shown as straight line. The fundamental component of the magnetic motive force (MMF) developed by the rotor PMs is expressed in Eq. (1) and the air-gap permeance is expressed in Eq. (2) below.

$$F_{PM1}(\theta,\theta_m) = F_1 \cos N_1(\theta - \theta_m)$$

$$= \frac{4}{\pi}\frac{h_{m1}}{\mu_m}B_r \cos N_1(\theta - \theta_m) \tag{1}$$

$$P_1(\theta) = P_{01} - P_{11}\cos(Z_s\theta) \tag{2}$$

where, N_1 is the pole pair numbers of the rotor PMs, Z_s is the stator slot number, θ_m is the rotor position and θ is the angular position in the air gap. h_{m1} is the thickness of the rotor PM. From Eq. (1) and Eq. (2), the air-gap flux density developed by rotor PMs is given by Eq. (3).

$$B_1(\theta,\theta_m) = F_{PM1}(\theta,\theta_m)P(\theta)$$

$$= \frac{4}{\pi}\frac{h_{m1}}{\mu_m}B_r \cos N_1(\theta - \theta_m)\left[P_0 - P_1\cos(Z_s\theta)\right]$$

$$= \frac{4}{\pi}\frac{h_{m1}}{\mu_m}B_r\left\{\begin{array}{l} P_{01}\cos N_1(\theta - \theta_m) \\ -\dfrac{P_{11}}{2}\cos\left[(N_1 - Z_s)\theta - N_1\theta_m\right] \\ -\dfrac{P_{11}}{2}\cos\left[(N_1 + Z_s)\theta - N_1\theta_m\right] \end{array}\right\} \tag{3}$$

The flux linkage within one stator pole range due to the rotor PM is given as:

$$\phi_1(\theta_m) = \left(r_1^2 - r_2^2\right)\int_0^{\pi/p} B(\theta,\theta_m)d\theta$$

$$= \left(r_1^2 - r_2^2\right)\frac{4}{\pi}\frac{h_{m1}}{\mu_m}B_r\left\{\frac{P_0}{N_1}\sin N_1(\theta - \theta_m)\right.$$

$$-\frac{P_1}{2(N_1 - Z_s)}\sin\left[(N_1 - Z_s)\theta - N_1\theta_m\right] \tag{4}$$

$$\left.-\frac{P_1}{2(N_1 + Z_s)}\sin\left[(N_1 + Z_s)\theta - N_1\theta_m\right]\right\}\Big|_0^{\frac{\pi}{p}}$$

where, P is the pole pair number of the stator windings, r_1 and r_2 are the outer radius and inner radius of the rotor PMs, respectively. When the pole-pair number of rotor PMs equals to the pole-pair number of the stator windings, namely $N_1 = p$, the flux density due to the flux modulation effect with $N_1 \pm N_s$ is negligible and there is no gear effect. To employ the flux modulation effect, the pole pair numbers should satisfy the relationship $N_1 - Z_s = \pm p$. Eq. (4) can be rewritten as:

$$\varphi_1(\theta_m) = \left(r_1^2 - r_2^2\right)\frac{4}{\pi}\frac{h_{m1}}{\mu_m}B_r\left(\frac{P_0}{N_1} \mp \frac{P_1}{2p}\right)\sin(N_1\theta_m)$$

$$= \Phi_1\sin(N_1\theta_m) \tag{5}$$

where, Φ_1 is the amplitude of windings flux linkage developed by the rotor PMs:

$$\Phi_1 = \left(r_1^2 - r_2^2\right)\frac{4}{\pi}\frac{h_{m1}}{\mu_m}B_r\left(\frac{P_0}{N_1} \mp \frac{P}{2p}\right) \tag{6}$$

The magnetic field of the rotor PMs is modulated by the stator slots. The rotor PMs and the stator slots consist of the first

set of flux modulation group. The rotor slots and the stator PMs inserted into the stator slots consist of the second modulation group. In the same way, the magnetic field excited by the stator PMs is modulated by the rotor iron segments. The pole pair number of the stator PMs is Z_s and the rotor pole number is N_1, the MMF developed by the stator PMs is expressed in Eq. (7) and the relevant air-gap permeance is expressed in Eq. (8).

$$F_{PM2}(\theta,\theta_m) = F_2 \cos Z_s \theta$$

$$= \frac{4}{\pi} \frac{h_{m2}}{\mu_m} B_r \cos Z_s \theta \qquad (7)$$

$$P(\theta) = P_0 - P_1 \cos N_1(\theta - \theta_m + \pi) \qquad (8)$$

The additional π in (8) is the angle difference between the rotor PMs and the rotor slots, and h_{m2} is the thickness of the stator PM. The air-gap flux density developed by stator PMs is expressed as:

$$B_2(\theta,\theta_m) = F_{PM2}(\theta,\theta_m)P(\theta)$$

$$= \frac{4}{\pi} \frac{h_{m2}}{\mu_m} B_r \left\{ \begin{array}{l} P_0 \cos Z_s \theta \\ -\dfrac{P_1}{2} \cos[(N_1 - Z_s)\theta - N_1\theta_m + N_1\pi] \\ -\dfrac{P_1}{2} \cos[(N_1 + Z_s)\theta - N_1\theta_m + N_1\pi] \end{array} \right\} \quad (9)$$

The flux linkage within one pole range of the stator windings due to the stator PMs is given as:

$$\varphi_2(\theta_m) = (r_1^2 - r_2^2) \frac{4}{\pi} \frac{h_{m2}}{\mu_m} B_r \left(\frac{P_0}{N_s} \pm \frac{P_1}{2p} \right) \sin(N_1\theta_m)$$

$$= \Phi_2 \sin(N_1\theta_m) \qquad (10)$$

The flux linkage of the stator winding is the superposition of these two fields and can be expressed as:

$$\varphi_s(\theta_m) = \varphi_1(\theta_m) + \varphi_2(\theta_m)$$

$$= (\Phi_1 + \Phi_2) \sin(N_1\theta_m) \qquad (11)$$

where, Φ_{PM1} is the flux linkage excited by the rotor PMs and Φ_{PM2} is the flux linkage excited by the stator PMs.

III. PERFORMANCE ANALYSIS WITH FEM

TABLE I
PARAMETERS OF the proposed machine

Parameters	AFDPM machine
Rated Power(kW)	3
Rated Speed (rpm)	600
Number of winding poles	4
Stator Outer diameter (mm)	200
Stator Inner diameter (mm)	80
Stator PM thickness (mm)	5
Number of stator slots	18
Number of stator small slots	5
Rotor outer diameter (mm)	205
Number of rotor poles	20
Rotor PM thickness (mm)	4.5
Remanence of magnets (T)	1.24
Rated speed (rpm)	600
Air gap length (mm)	0.5
Stack length (mm)	45

TABLE I shows the specification of the models. With 3d-FEM, the machine performance is analyzed. The flux density distribution of the AFDPM machine is shown in Fig. 4. To illuminate the flux density distribution clearly, the top part of the rotor is concealed. Fig. 5 shows the flux linkage of one phase of stator windings. To verify the Vernier theory conducted in Part II, the flux linkage developed by the rotor PMs, stator PMs and the superposition flux linkage are shown respectively. The solid line is the superposition flux linkage, the broken line is the flux linkage developed by the stator PMs and the dotted line is the flux linkage developed by the rotor. As seen from Fig. 5, the flux linkage developed by the stator PMs and rotor PMs have the same phase and the superposition flux linkage is their linear summation.
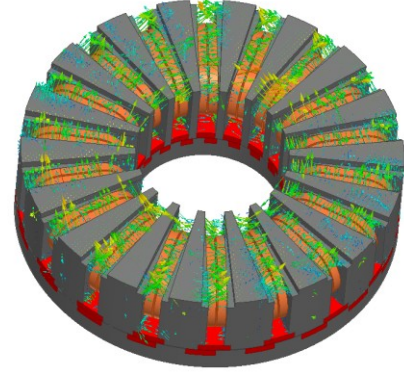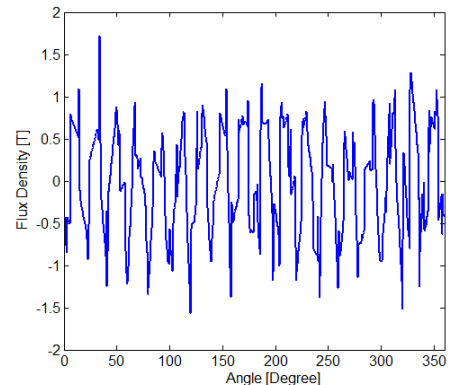

Fig. 4 Flux density distribution of the AFDPM machine

A. Airgap Flux Density Distribution

Fig. 5 and fig.6 show the computed flux distribution in the airgap. The axial flux density due to the stator PMs, as well as their space harmonic spectra, are shown respectively in figs. 5(a) and figs. 5(b). The axial flux density due to the outer winding in the airgap, as well as their space harmonic spectra, are shown in Figs. 6(a) and 6(b), respectively. It is easy to see that the 2 pole-pair harmonic is smaller than the 18 pole-pair harmonic but larger than other harmonics because of the vernier effect. The 2 pole-pair harmonic is the functional harmonic to couple with the stator winding. The axial flux density due to the inner stator PMs, as well as their space harmonic spectra, are shown respectively in Figs. 6(a) and figs.6(b) show the axial flux density due to the rotor stator PMs and its space harmonic spectra.
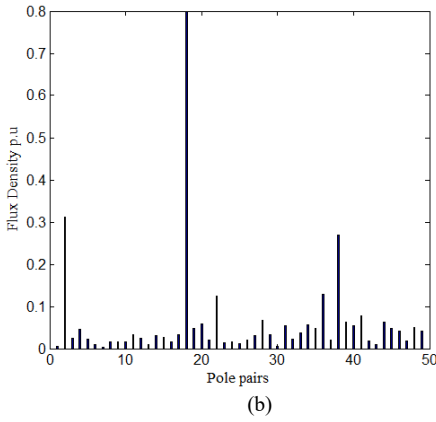

(a)

(b)

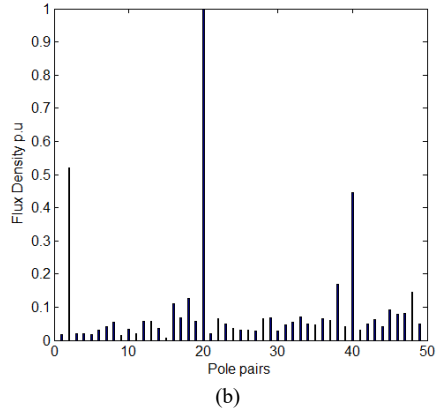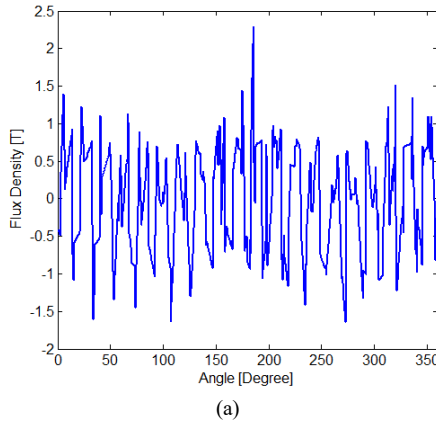Fig. 5 Flux density distribution of the AFDPM machine

(a)

(b)

Fig. 6 Flux density distribution of the AFDPM machine

B. Benefit of the Dual PM structure

The no-load back EMF is simulated at 600 rpm and shown in Fig. 7. In accordance with the flux linkage waveform, the solid line is the total no-load back EMF of the AFDPM machine. The broken line is the back EMF excited by the stator PMs and the rotor PMs are considered as vacuum. The back EMF excited by stator PMs is a little larger than the back EMF excited by the rotor PMs. It is because that the stator PMs is thicker than the rotor PMs as shown in TABLE I. The dotted line is the back EMF excited by the rotor PMs and the stator PMs are considered as vacuum. The additional broken dot line is the back EMF of a conventional AFVPM machine. The structure of the conventional AFVPM machine is shown in Fig. 8. With same rotor pole pair number, and stator slot number, the major peripheral dimensions of the AFVPM machine are the same as the AFDPM machine, except the PMs are only mounted on the rotor without slots. The no load back EMF of the novel stator and rotor dual PM structure is much larger the conventional Vernier structure in the same size as shown in Fig. 9. It indicates the novel structure has higher power density and torque density than the conventional AFVPM machine with the same electric loading and magnetic loading. The no load back EMF is increased from 80V of the AFVPM machine to 120V of the AFDPM machine.
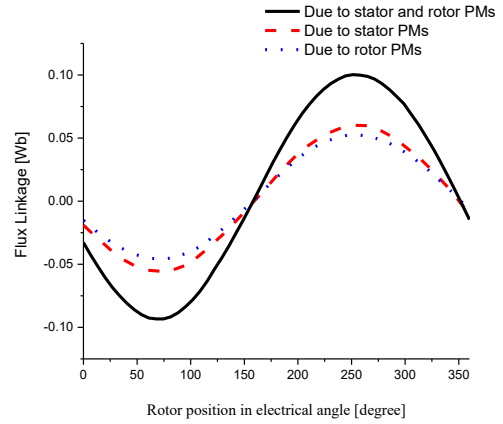

Fig. 7 Flux linkage of the stator windings with different rotor position
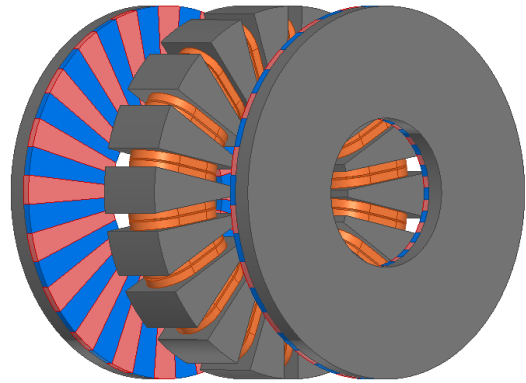

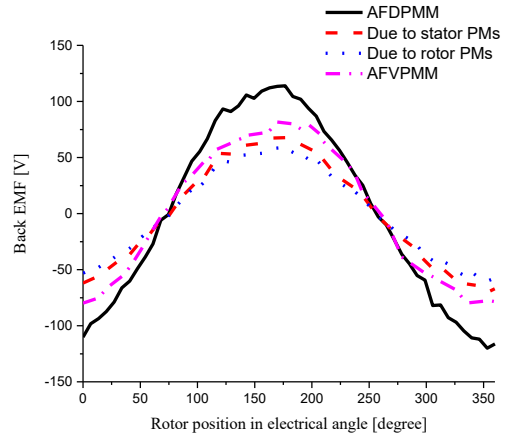Fig. 8. Structure of a conventional axial flux vernier PM machine.

Fig. 9. No-load back EMF of the stator windings with different rotor position.

Fig.10 shows the maximum torque with different armature current. The torque-current characteristic is not a straight line for both AFDPM machine and AFVPM machine. The reason is that the armature reaction cause the magnetic satuation when the current density is high. Same as the no-load back EMF, the torque of the AFDPM machine is also higher than the AFVPM machine with the same winding current.
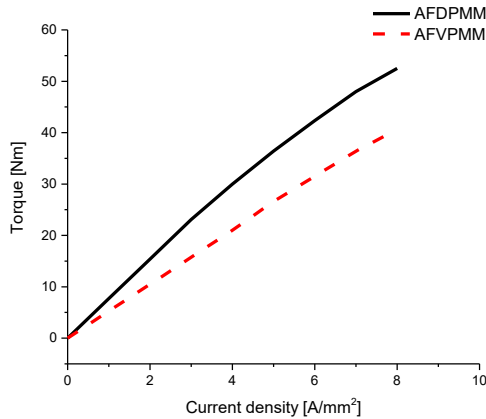

Fig. 10. Maximum torque with different armature current density.

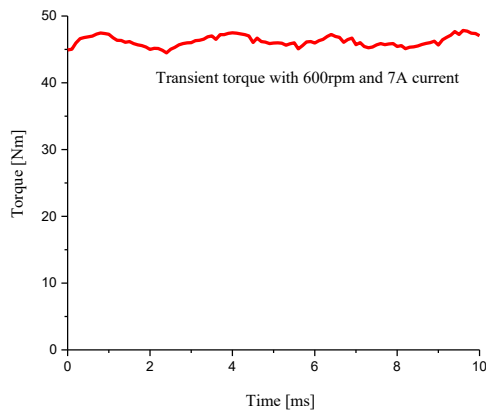*C. Transient Torque and Efficiency*

Fig. 11. Transient torque at 600 rpm.

Fig. 11 shows the steady torque waveform of AFDPM machine with 7 A current density and 600 rpm rotation speed. The torque ripple is 5Nm (peak to peak). Due to the dual PM structure, it is lager than the torque ripple of convention AFPM machines. This is a major drawback of the AFDPM machine. Using the multilayer structure, the torque ripple of the AFDPM machine can be suppressed. Fig. 12 shows the core loss of the AFDPM machine with full load condition. In full load condition, the copper loss of the AFDPM machine is 72W and the core loss 139W. Considering the stray loss is 1%, the efficiency of the AFDPM machine is 92.4% in the full load condition.
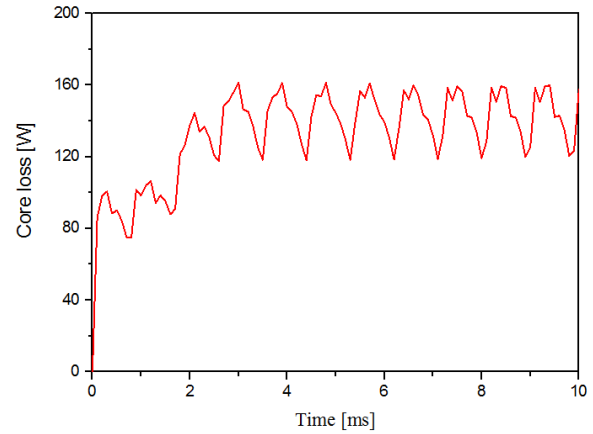

Fig. 12. Core loss with full condition.

IV.   CONCLUSION

In this paper, a novel structure of axial flux stator and rotor dual PM machine is proposed. The novel machine has the merits of high power density and torque density at low speed. It is suitable for direct drive applications with limited space such as in-wheel electrical propulsion system. The flux modulation effect is formulated and working principle is explained. 3d-FEM is employed to prove the accuracy of the model and the transient and static performance of machine is analyzed. Compared with conventional axial flux PM machines, the torque density is improved by around 20% as shown in the simulation result.

REFERENCES

[1] K. T. Chau, C. C. Chan, and C. Liu, "Overview of permanent-magnet brushless drives for electric and hybrid electric vehicles," *IEEE Trans. Indus. Electron.,* vol. 55, no. 6, pp. 2246–2257, Jun. 2008.

[2]   Z. Q. Zhu and D. Evans, "Overview of recent advances in innovative electrical machines—With particular reference to magnetically geared switched flux machines," in *Proc. International Conference on Electrical Machines and Systems,* Hangzhou, China, Oct. 2014, pp. 1–10.

[3] T.M. Jahns, "The expanding role of PM machines in direct-drive applications", in *Proc. International Conference on Electrical Machines and Systems,* Beijing, China, 2011, On page(s): 1 - 6

[4] M. Cheng, K. T. Chau and C. C. Chan, "Design and analysis of a new doubly salient permanent magnet motor, " *IEEE Trans. Magn.*, vol. 37, no. 4, pp.3012 -3020 2001

[5] M. F. Rahman , M. E. Haque , L. Tang and L. Zhong, "Problems associated with the direct torque control of an interior permanent-magnet synchronous motor drive and their remedies," *IEEE Trans. Ind. Electon.*, vol. 51, no. 4, pp.799 -809 2004

[6] A. M. El-Refaie and T. M. Jahns, "Comparison of synchronous PM machine types for wide constant-power speed operation: Converter performance," *IET Electr. Power Appl.,* pp. 217–222, 2007.

[7] Y. Wang, S. L. Ho, W. N. Fu and J. X. Shen, "A Novel Brushless Doubly Fed Generator for Wind Power Generation," *IEEE Trans. Magn.*, vol. 48, no. 11, pp. 4172-4175, November 2012.

[8] C. H. Lee, "Vernier motor and its design," *IEEE Trans. Power App. Syst.,* vol. PAS-82, no. 66, pp. 343–349, Jun. 1963.

[9] A. Ishizaki, T. Tanaka, K. Takasaki, and S. Nishikata, "Theory and optimum design of PM Vernier motor," in *Proc. international conference on electrical machines and drives,* Piscataway, New Jersey, 1995, pp. 208–212.

[10] B. Kim and T. Lipo, "Operation and design principles of a PM vernier motor," *IEEE Trans. Ind. Appl.,* vol. 50, no. 6, pp. 3656–3663, Nov./Dec. 2014

[11] S. Niu, S. L. Ho, W. N. Fu, "A novel stator and rotor dual permanent magnet Vernier motor with space vector pulse width modulation," *IEEE Trans. Magn.*, vo.l 50. no. 2, pp.805-808, Feb 2014.

[12] T. S. Kwon, S. K. Sul, L. Alberti, N. Bianchi, "Design and control of an axial flux machine for a wide flux-weakening operation region," *in Conf. IEEE Industry Applications Annual Meeting 2007*, New Orleans, Louisiana, 2007, pp. 2175-2182.

[13] H. Tiegna , A. Bellara , Y. Amara and G. Barakat, "Analytical modelling of the open-circuit magnetic field in axial flux permanent magnet machines with semi-closed slots," *IEEE Trans. Magn.*, vol. 48, no. 3, pp.1212 -1226 Nov. 2012

[14] S. Huang , J. Luo , F. Leonardi and T. A. Lipo, "A comparison of power density for axial flux machines based on general purpose sizing equations," *IEEE Trans. Energy Convers.*, vol. 14, no. 2, pp.185 -192 1999

[15] F. G. Capponi, G. De Donato, and F. Caricchi, "Recent advances in axial-flux permanent-magnet machine technology," *IEEE Trans. Ind. Appl.,* vol. 48, no. 6, pp. 2190–2205, Nov./Dec. 2012.

Xingjian Li was born in Chaoyang, Liaoning, China, in 1995. He is currently studying at Xi'an Jiaotong Liverpool University for his bachelor degree in electrical engineering.
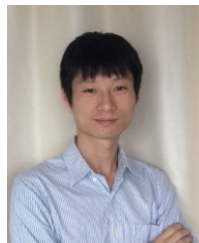
Yunchong Wang received his B.Sc and M.Sc degrees, from the school of Electrical Engineering, Zhejiang University, Zhejiang, China, in 2010 and 2013, respectively. He is currently working toward the Ph.D. degree in the department of Electrical Engineering from The Hong Kong Polytechnic University. His research interests include electrical motor design and control, electrical vehicles and renewable energy conversion system.
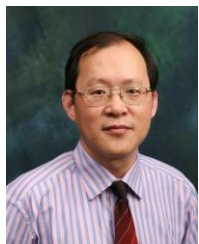
W. N. Fu received his BEng in Electrical Engineering, Hefei University of Technology, Hefei, China in 1982 and MEng in Electrical Engineering, Shanghai University of Technology, Shanghai, China in 1989. He obtained his PhD in electrical engineering from The Hong Kong Polytechnic University in 1999.

He is now a Professor in The Hong Kong Polytechnic University. Before joining the university in October 2007, he was one of the key developers at Ansoft Corporation in Pittsburgh, USA. He has about seven years of working experience at Ansoft, focusing on the development of the commercial software Maxwell. He has published 184 papers in refereed journals. His current research interests mainly focus on numerical methods of electromagnetic field computation, optimal design of electric devices based on numerical models, applied electromagnetics and novel electric machines.